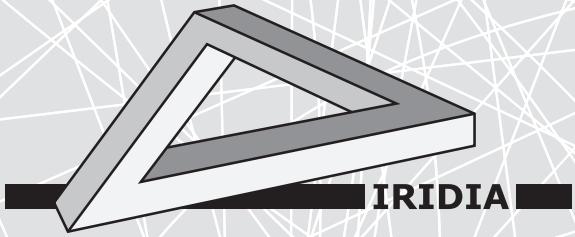


**Université Libre de Bruxelles**

*Institut de Recherches Interdisciplinaires*
*et de Développements en Intelligence Artificielle*

# An Open Localisation and Local Communication Embodied Sensor

Álvaro Gutiérrez, Alexandre Campo, Marco Dorigo,
Daniel Amor, Luis Magdalena and
Félix Monasterio-Huelin

**IRIDIA – Technical Report Series**

Technical Report No.
TR/IRIDIA/2008-019

September 2008

**IRIDIA – Technical Report Series**
ISSN 1781-3794

Published by:

IRIDIA, *Institut de Recherches Interdisciplinaires et de Développements en Intelligence Artificielle*
Université Libre de Bruxelles
Av F. D. Roosevelt 50, CP 194/6
1050 Bruxelles, Belgium

Technical report number TR/IRIDIA/2008-019

Revision history:

TR/IRIDIA/2008-019.001 September 2008

# An Open Localisation and Local Communication Embodied Sensor

Álvaro Gutiérrez[1], Alexandre Campo[2], Marco Dorigo[2],
Daniel Amor[3], Luis Magdalena[4] and Félix Monasterio-Huelin[1]

[1] ETSIT, Universidad Politécnica de Madrid, Madrid, Spain
aguti@etsit.upm.es, felix.monasteriohuelin@upm.es
[2] IRIDIA, CoDE, Université Libre de Bruxelles, Bruxelles, Belgium
{acampo,mdorigo}@iridia.ulb.ac.be
[3] RBZ Robot Design S.L., Madrid, Spain
daniel@rbz.es
[4] European Centre for Soft Computing, Asturias, Spain
luis.magdalena@softcomputing.es

September 2008

**Abstract**

Although wireless, mainly radio, communications are universally used in sensor networks, no localisation information is offered in an unstructured environment, without modifying or characterising the surroundings. In this paper we describe a localisation and local communication sensor which allows situated agents to communicate locally obtaining at the same time the range and bearing of the source of emission without the need of any external system. The information is correlated in the board without the need of an external reference point. The system is based on infrared communications with frequency modulation and two interconnected systems for data and power measurement. The sensor operates at a high data rate in a range that can be modulated and proves to be reliable. Due to the open hardware license, it allows the research community to replicate and adapt at low cost the sensor board for any other needs.

## 1 Introduction

Sensor networks are currently used in many civilian application areas such as environment monitoring [18], security systems [12], home automation [10], traffic control [3], medical applications [6] or efficient energy consumption [5]. These networks consist of spatially distributed autonomous devices using sensors to collectively monitor and cooperate to resolve specific tasks [1, 7]. Sensor networks are built with one or more sensors in each node. A node is typically equipped with a wireless communication device, a controller and an energy source. Each node has limited capabilities but coordinating with the rest of the network's nodes, they have the ability to complete a given task. Thus, a sensor network can be described [1] as a collection of sensor nodes that co-ordinate their actions to carry out collective tasks.

But what does this coordination mean? Typical applications, as those mentioned above, are related to static networks where the sensors are placed at fixed points and the location environment is modelled once the sensors have been positioned. In these examples, only abstract communication is needed where some IDs and data information (e.g., temperature, humidity) are offered to the network. The distributed network is in charge of acquiring the data and proceeding to the control task. The collaboration is mainly limited to send sensory information to the network, where a

main processor or the network itself will process them to carry out its task. The network has a predefined nodes map, and only information of those nodes is acquired by the network.

However, in a world where intelligent ambients and autonomous systems are converging, communication starts to play an important role not only with the contents of messages but also with additional characteristics in embodied communication, where the message is a function of the location of the communicating agents. Previous works in location and local communication [20, 8] have addressed this problem, but usually a model of the environment, location of the agents or an explicit knowledge has to be programmed into the nodes or agents. In wireless mobile applications, nodes usually calibrate and triangulate their positions according to a model obtained in the design process [11, 16]. In home automation sensor networks, a map of the rooms and sensors locations [4] is predefined and programmed on the network, while in security mobile systems a map of the environment is offered to the agent which will employ fusion technics for locating itself and their teammates [17]. These implementations allow an accurate description of a specific environment but if the network moves to other new places all the modelling efforts must be repeated.

Following modern artificial intelligence approaches [2, 19] new functionalities and autonomies could be given to the networks, which should discover the environment and self-organise their topology. The agents (mobile or static) should identify their location according to their body and situation [14, 21]. This self-localisation will offer the network autonomous capabilities that will be shared between the nodes. The situated communication that is created by the network itself allows the nodes to be moved from one place to an other, and to create its own sensory map.

Previous works have been implemented in the localisation and communication field. In some cases the systems are implemented in large-scale nodes [9, 15] and miniaturisation is extremely difficult due to its electronics. In others [13], there is not enough information to replicate the system or the system is too expensive to design [15]. For these reasons replication or extension of previous experiments are difficult to achieve.

In this work we present an open hardware communication system that allows limited range communication and localisation of emitters by receivers. This board has been designed for robotics tasks but could be applied to many other applications such as industrial manufactures, weather stations, security systems, and so on. Due to the different board usages, we focus on the hardware system abstracted from any specific application. The system provides a high communication rate in a range that can be modulated and proves to be reliable. The system gets the data and extracts at the same time the range and bearing from the communication. All the specifications of the board are available under open hardware license and due to its low production cost (200 euros) the board is easily reproducible.

# 2 Localisation and Communication System

The designed board (see Figure 1) is controlled by its own processor. Each board includes 12 sets of IR emission/reception modules. Each of this modules is equipped with one infrared emitting diode, one infrared modulated receptor and one infrared photodiode[1]. The modules, as shown in Figure 2, are nearly uniformly distributed on the perimeter of the board; so, the distance between them is approximately 30°.

## 2.1 Power Supply Module

The board can be powered from 2.5 V to 6 V. Once the board is switched on, three isolated power lines are created: One for the digital system, one for the analog and the last one for the emission module. The three power lines are obtained from two different supplies.

The first power supply is in charge of the emission module. This supply is based on a low dropout linear regulator which allows a voltage variation between 0.8 V and 3.3 V (see Figure 3). This power variation permits the module to modify the emission range. The regulator is connected to a digital SPI potentiometer which varies the load of the ADJ pin modifying the output of the

[1] For an exhaustive description of the board see http://www.rbz.es/epuck/.

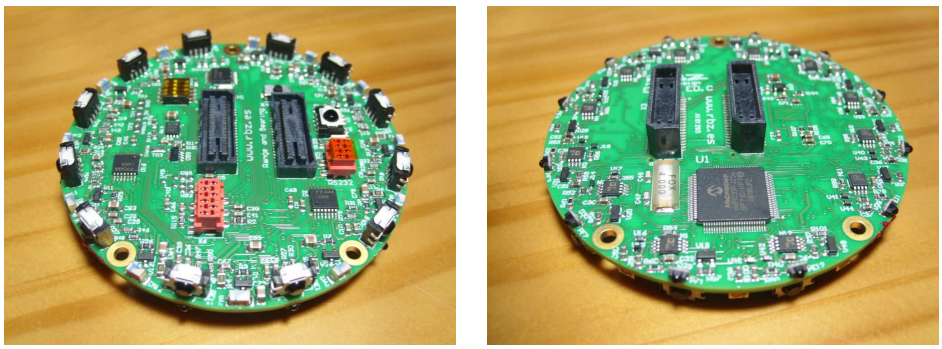

(a) (b)

Figure 1: (a) Top and (b) bottom view of the localisation and local communication board.

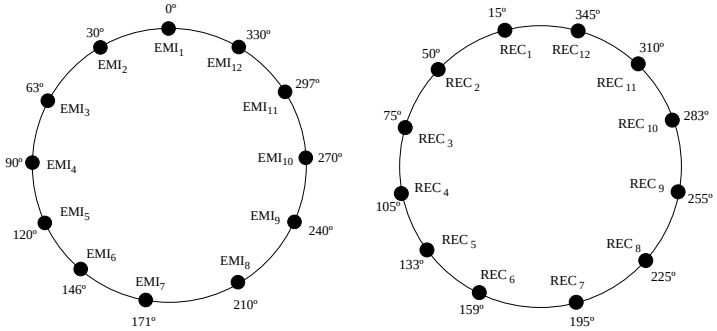


(a) (b)

Figure 2: (a) Emitters and (b) Receivers distribution around the perimeter of the board.

source. Due to this digital variable resistor the emission range and power consumption can be software controlled.

*R102* and *R114* are 15 KΩ resistors, and potentiometer *D53* modifies its value from 0 Ω to 100 KΩ with an 8 bits SPI frame, so 256 levels of approximately 390 Ω are managed. Resistors $R102 + D53$ and *R114* form the resistor divider network necessary to set the output voltage. With this configuration, $V_{emis}$ follows Equation 1:

$$V_{emis} = V_{adj} \frac{(R102 + D53) + R114}{R114} \tag{1}$$

where $V_{adj}$ has a nominal voltage of 0.4 V. $V_{emis}$ minimum value of 0.8 V is achieved for *D53*=0 Ω, and maximum value of 3.46 V for *D53*=100 KΩ

The second power supply is in charge of the rest of the electronics including the micro controller. Analog and digital lines, both of 3.3 V, are separated and short circuited just in one point to reduce noise.

The power consumption of the board depends on the emission power supply. Table 1 shows the consumption characteristics of the board for different values of the adjustable power supply during a 50% duty cycle of the emission signal.

## 2.2 Emission Module

The emission module is composed of 12 different emitters. Each sensor set is composed of a narrow beam infrared led and logic gates to create the modulation as the one shown in Figure 4. The infrared leds have its nominal half intensity angle at ±20°, a 100 mA forward current, a maximum power consumption of 180 mW and a nominal switching time of 12 ns.

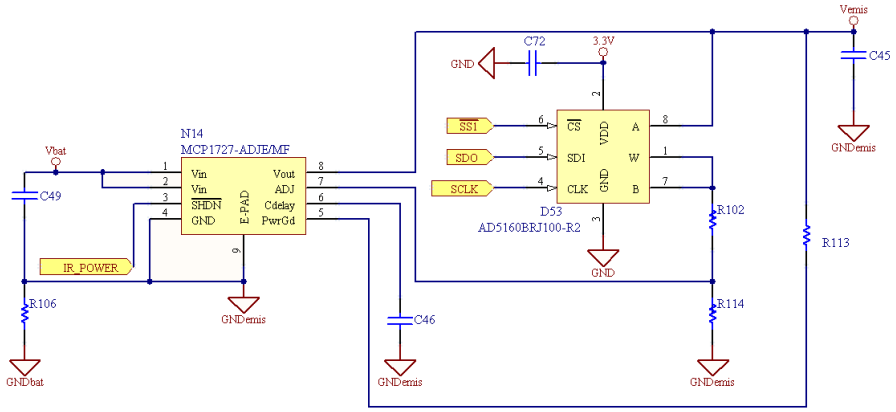


Figure 3: Depiction of the power supply in charge of the emission module.

| $V_{emis}$ | Min (mW) | Nominal(mW) | Max(mW) |
|---|---|---|---|
| 0% | 70 | 74 | 80 |
| 10% (0.8 V) | 110 | 114 | 119 |
| 50% (2.13 V) | 392 | 396 | 400 |
| 100% (3.46 V) | 674 | 679 | 683 |

Table 1: Consumption characteristics of the board.

Communication is based on frequency modulation with data at 10 KHz modulated over a carrier of 455 KHz (see Figure 5 for more details). Finally a FET transistor is added to power on the emitter.

The modification of the $V_{emis}$ power supply changes the current that pass trough the emitter modifying the emission range. For a minimum value of 0.8 V, a 40 cm range is achieved while the maximum range is approximately 6 m for $V_{emis}$=3.46 V.

## 2.3 Reception Module

The reception system is divided in two different modules. A first module is in charge of the data reception while the second one takes care of power signal intensities. The division of the two modules allows the board to work in both data and embodied communication separately. In the first one, the board is able to work as a simple communication system, where the data are demodulated and received without the extraction of the power source location. The second module starts measuring the intensity of infrared signals during the reception of a frame. To ensure a proper measure of the signal intensity, power and demodulating sensors must have the same orientation and are therefore positioned on the top of each other.

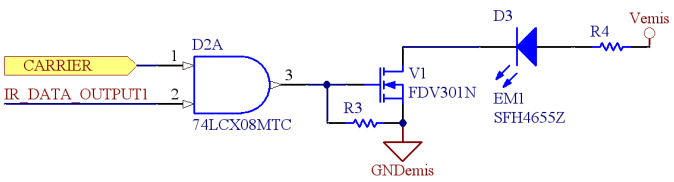


Figure 4: Depiction of one emission module.

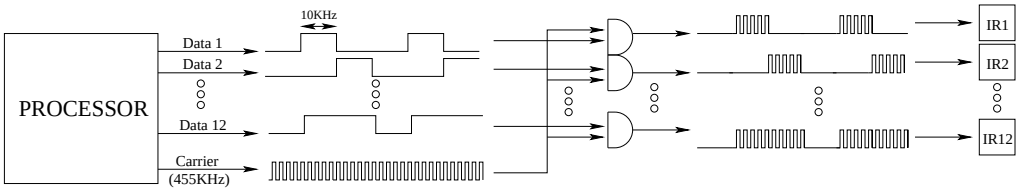


Figure 5: Board emission diagram.

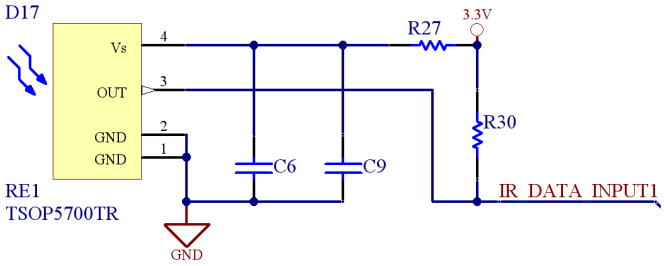


Figure 6: Depiction of one data reception module.

The data reception module is based on a miniaturised infrared receiver for remote control (see Figure 6). The sensor is packed with a PIN diode and a preamplifier, and the demodulated output signal can directly be decoded by a microprocessor. The receptor demodulates signals with a 455 KHz carrier and data rate is up 20 Kbits/s. The signals are received trough digital inputs in the microcontroller.

The power reception module is based on a PIN diode and two operational amplifiers. The diagram shown in Figure 7a shows a peak detector system with a $R54/R51$ gain. When the photodiode starts receiving infrared signals, the circuit starts charging capacitor *C50*. Once the signal is exhausted, the system keeps the voltage in the capacitor (if no leak currents are taken into account). If a higher strength signal arrives to the diode, it will continue charging the capacitor. If the signal arrived has a lower intensity than the actual value stored in the capacitor, the peak detector will keep its value (see an example in Figure 7b). The outputs from the peak detector face 12 analog to digital converters in the microcontroller. Finally, a hardware reset based on a FET transistor ($V19$) is added to the circuit for discharging the capacitor. The resets are managed trough 12 independent output pins. The complementary activities of the data and power reception modules are sketched in Figure 8.

## 2.4 Communication Module

The board has been designed to be a slave module of a main processor system. As explained in the Introduction Section, the design has been carried out for an autonomous robot, but the board can be used in many other domestics or intelligent ambient environments. For this purpose, two buses, I2C and RS232, have been designed for the communication with the board.

In the I2C communication the board acts as slave of the main processor system. The board takes care of the requests of transmission and is continuously checking for incoming frames. The master board should be pulling continuously the board to check if any communication has been received.

In the serial port communication, interruptions are enabled in both directions. The master board is able to send orders of transmission or range modifications. Once a frame is received by the communication board, it interrupts the master sending the data received and the estimated angle and distance to the source of emission.

In both communication types the master has the control of the emission range. The modification of the power supply output is made online which results on a instantaneous change of the

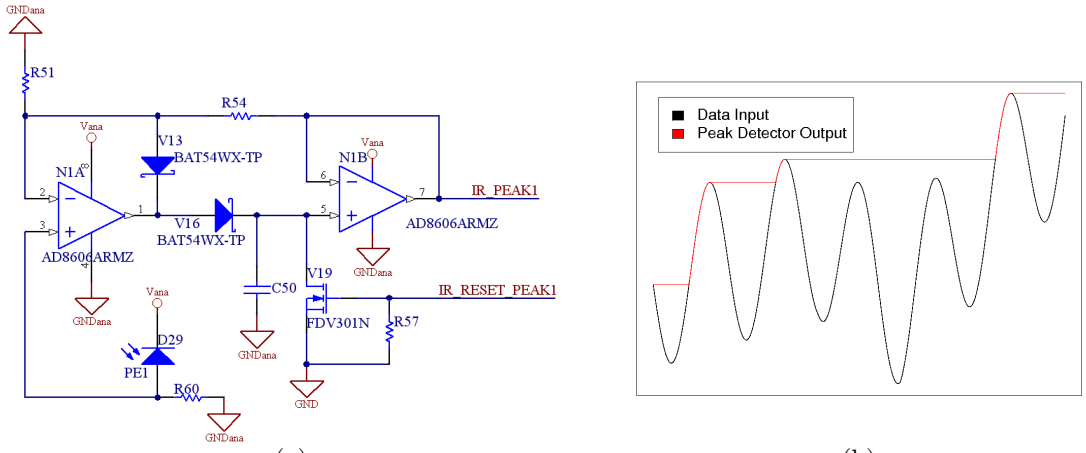


Figure 7: (a) Peak detector functionality. (b)Depiction of one power reception module.

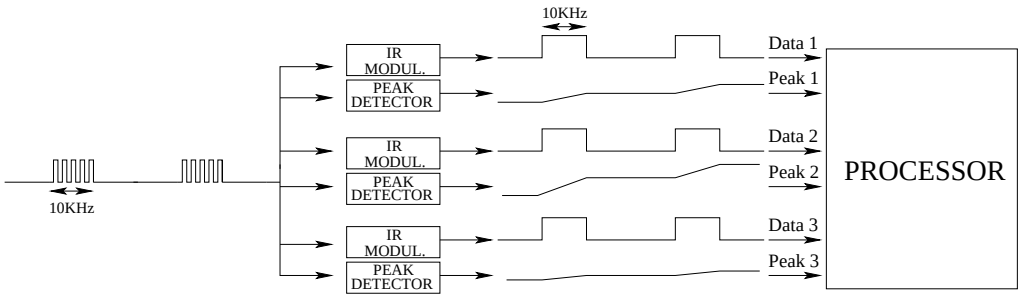


Figure 8: Depiction of a reception diagram.

emission range.

## 2.5 Software Implementation

Once the board is powered, a sequence of timers starts. At the very beginning all the input/output ports and analog to digital ports are defined. After the definition of the peripherals the I2C and serial port communications are started. Finally, the emission and reception software modules are initialised.

The emission software is linked to the communication system. Once the board is initialised, the range of emission is defined to its maximum value, and it will change after a master board order. After defining the range, a pulse-width modulation (PWM) timer is initialised at a 1.09 $\mu$s. This timer creates the carrier of the emission module which will not be stopped until the board is powered down. A second timer in charge of the data frame rate is initialised and interrupts each 100 $\mu$s which implies a 5 Kbits/s data rate. Data rate is half of the timer timing because messages are sent based on a Manchester code, which is used to obtain the same signal power level for all the messages. Therefore, the reception module will receive the same signal strength for different messages sent at the same distance. Each interruption of this timer takes a buffered data and sends it to the hardware gates for its transmission. Data for transmission are stored in a buffer correctly structured according to the hardware pinout. Three different types of transmission can be asked to the communication board:

- **All the sensors transmit the same data**: One instruction is sent to the board, along with the data to transmit.

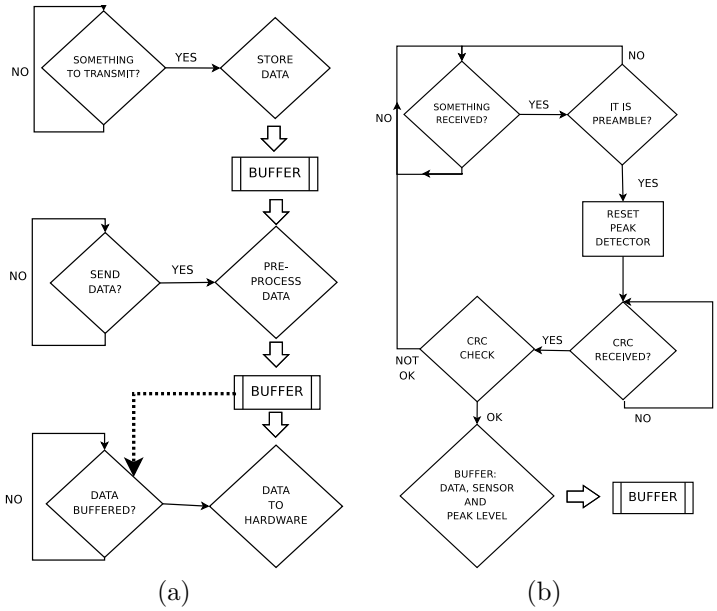


Figure 9: Block diagram of the (a) software emission module and (b) software reception module.

- **Only some sensors transmit data**: One instruction for each sensor must be sent to the board. Data and sensor number must be also provided to the board. After all the sensors have been programmed, a "send" instruction must be sent to the board.
- **Different sensors transmit different data:** One instruction for each sensor must be sent to the board. Data and sensor number must be also provided to the board. After all the sensors have been loaded, a "send" instruction must be sent to the board.

Once a transmission order arrives, the communication module is in charge of decomposing the data for the different sensors. The module introduces a preamble (2 bits), the data (8 bits) and a CRC (2bits), in a Manchester code and specifically re-ordered to face the hardware pinout. If continuous data wants to be transmitted, the communication module buffers all the data one after the other, where the number of messages is transparent for the transmission timer.

The reception software is continuously checking if a message arrives. Once the preamble of a frame is detected by an infrared data receiver, it resets its associated peak detector. The software continues receiving the data and CRC, while the peak detector is charging the capacitor with the signal level received. If the frame has correctly arrived, the peak detector level is read and stored in a buffer. As the aperture of the receiving sensor is wide, it is likely that more than several sensor receive the same data at the same time. The information given by the different peak detectors is used to calculate the orientation and distance to the source of transmission. These two values are then stored in a buffer to be sent to the master module. Figure 9 shows a block diagram of the emission and reception modules.

# 3 Model Description

Due to the hardware design, one single transmission is likely to be detected by several infrared sensors. For getting the correct location information, an internal data fusion must be carried out before supplying data to the master module. Figure 10 shows an example of a reception diagram. We observe that several sensors are receiving the same information but there is a signal strength difference between the sensors. In Figure 10a we observe that the source of emission is facing sensor $I_{S_6}$ while in Figure 10b the orientation of the source is in some point between $I_{S_8}$ and $I_{S_9}$.

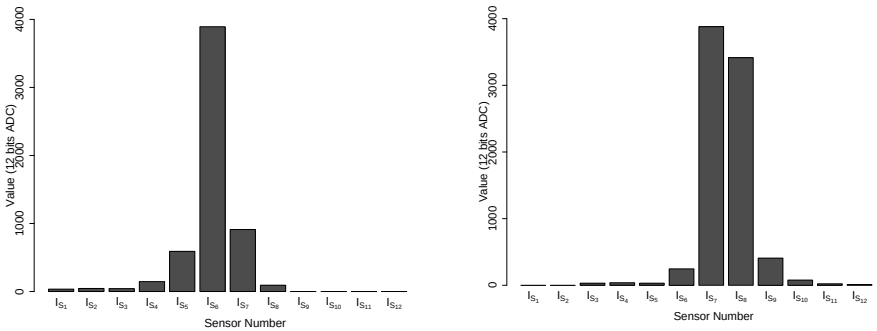


Figure 10: Sensory map for two different reception frames. (a) The emitter is approximately facing a reception sensor. (b) The emitter is in some point in between two reception sensors.

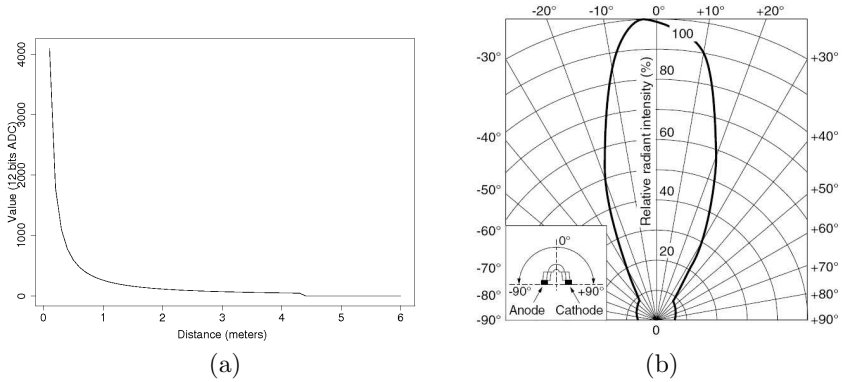


Figure 11: (a) Reception values for different distance transmissions when emitter and receiver sensors are facing each other. (b) Radiation diagram for the PIN diode of the peak detector. (Obtained from the PD100MF0MPx Datasheet).

For getting a more accurate measure on the bearing we implement a linear combination between the two sensors with highest power signal following Equation 2:

$$\widetilde{\xi} = \frac{\phi_{max_1}\widehat{\nu}_{max_1} + \phi_{max_2}\widehat{\nu}_{max_2}}{\widehat{\nu}_{max_1} + \widehat{\nu}_{max_2}} \tag{2}$$

where $\widetilde{\xi}$ is the estimated angle, $\phi_{max_1}$ and $\phi_{max_2}$ are the orientation angles of the two maximum reception value sensors and $\widehat{\nu}_{max_1}$ and $\widehat{\nu}_{max_2}$ are the received values on both sensors.

To estimate the distance of the emitter, the same spatial problem arises. It is difficult to determine accurately the distance from a single sensor. Instead, we use a linear combination based on the estimated angle and the estimated distances provided by the two maximum reception sensors. To this end, we have devised an empiric relationship between the ADC values and the distance when the emitter and receiver sensors are facing each other as shown in Figure 11a. As the receptor sensors have a maximum sensibility angle at $-3°$ which decrease according to Figure 11b, the relationship between the ADC values and the distance must be extended to a 3D graph as shown in Figure 12. Following this graph we calculate the estimated distances $\widetilde{\rho}_{max_1}$ and $\widetilde{\rho}_{max_2}$ from the emitter to each of the two maximum sensors from the received ADC values $\widehat{\nu}_{max_1}$ and $\widehat{\nu}_{max_2}$ respectively.

Applying the law of cosines, we devise a relationship to calculate two estimated distances $\lambda_{max_i}$

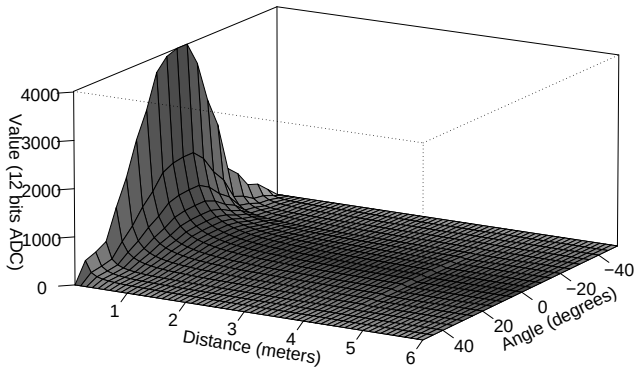


Figure 12: Reception values for different distance and angle transmissions.

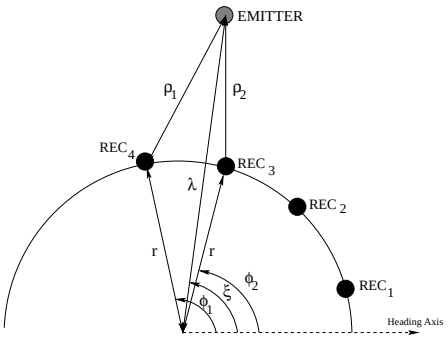


Figure 13: Reception diagram for a specific location and its distance to the different sensors.

from the centre of the board to the emitter following Equation 3 (see also Figure 13):

$$\widetilde{\lambda}^2_{max_i} - 2r\widetilde{\lambda}_{max_i}\cos\left(|\widetilde{\xi} - \phi_{max_i}|\right) + \left(r^2 - \widetilde{\rho}^2_{max_i}\right) = 0, \quad i = 1, 2 \tag{3}$$

where $r$ is the board radius.

We obtain the estimated distance $\lambda$ of the emitter by averaging out $\lambda_{max_i}$ as shown in Equation 4:

$$\widetilde{\lambda} = \frac{\widetilde{\lambda}_{max_1} + \widetilde{\lambda}_{max_2}}{2} \tag{4}$$

# 4 Experimental Section

A number of tests have been run to characterise the localisation and communication system. One emitter and one receiver board are placed in a free-obstacle environment from 10 cm to 6 m, in 10 cm interval as shown in figure 14. At each distance the board is placed at 8 different orientations from the emitter (each 45°) to avoid bias on the emitter transmission. The emitter stays in place while the receiver is rotated at a 10° interval in each position. At each position, the receiver waits till 100 messages are received and stores its 12 sensors peak values. We have repeated this test for 60 linear positions, 8 orientations, and 36 angular rotations for 10 different boards.

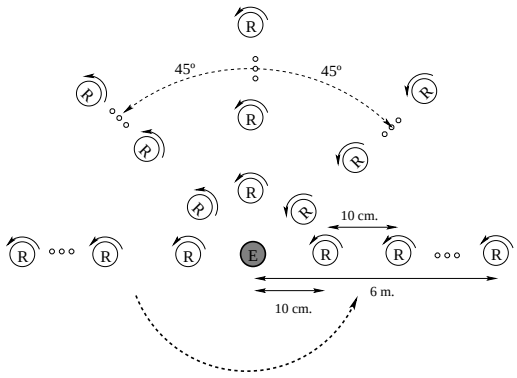


Figure 14: Physical arrangement of the boards for the experiments.

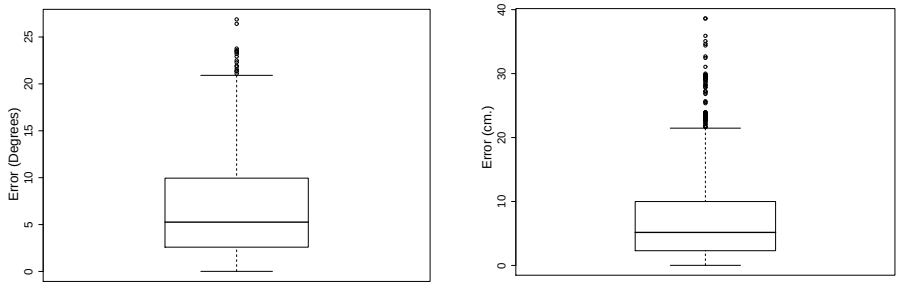


(a) (b)

Figure 15: Algorithm performance for calculating (a) the angle and (b) the distance error. Each box comprises observations ranging from the first to the third quartile. The median is indicated by a horizontal bar, dividing the box into the upper and lower part. The whiskers extend to the farthest data points that are within 1.5 times the interquartile range. Outliers are shown as dots.

The error for each range and bearing of the receiving board over all measures was calculated. The error on the bearing was 6.69° on average and 26.87° in the worst case. The error on the range was 7.18 cm on average and 38.62 cm on the worst case (see Figure 15 for the error distribution). The variation of the distance error with respect the range is shown in Figure 16a. We observe errors of 1 cm on average for 10 cm transmission distance and 20 cm on average for 4 m. Finally Figure 16b shows the error rate of the communication system. From 0 to 3 meters there are no missing frames. For distances higher than 3 meters the reception error rate starts increasing up to 6 meters, where frames are not received anymore.

Notice that for distances higher than 4 meters there is no range and bearing estimation, while data is received up to 6 meters. This is due to the sensibility of the photodiode sensors. This means that if the emitter is farther than 4 meters, the board will receive the data but it will not be able to calculate the distance to the emitter. The board will return the data, a bearing estimate calculated using the position of the data receptors which have received a correct frame, and the range will be left as a *too far* tag.

# 5 Conclusions

In this paper we have described the design of an open board for localisation and local communication. We show the different communication modules and their principal characteristics.

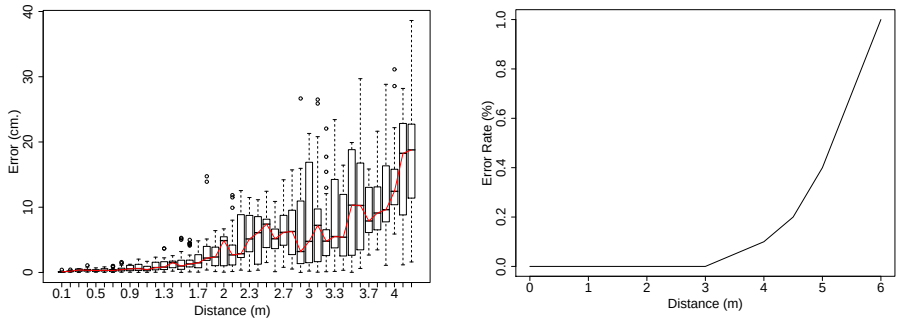


(a) (b)

Figure 16: (a) Standard deviation of the distance calculations respect to the real range. (b) Error rate of the communication system.

The system provides a high communication rate of 5 Kbits/s with a frequency modulation which allows better robustness to light conditions. The range from 0 to 6 meters can be modified by software in real time. The system gets the data and extracts range and bearing from the communication at the same time. The board operates with high reliability at distances below one meter with a maximum error of 1 cm in range and 2° in bearing. For longer distances performance degrades gracefully with a maximum error of 38.62 cm in range and 26.87° in bearing at 6 meters.

Although the board has been designed for robotics tasks, it can be easily reused in different applications such as smart sensors, intelligent ambients, home automation, *etc...* Due to the open hardware license under which the board is released, along with the full documentation and the low cost of production, this new range and bearing board provides researches with a new and versatile communication tool.

## Acknowledgements

Alexandre Campo and Marco Dorigo acknowledge support from the F.R.S.-FNRS. This work was partially supported by the RBZ Robot Design S.L. Company, by the *ANTS* project, an *Action de Recherche Concerté* funded by the Scientific Research Directorate of the French Community of Belgium and by the *Ministerio de Educación y Ciencia* of Spain, within the *Plan Nacional de I+D+I 2007-2010. (Gestión de la Demanda Eléctrica Doméstica con Energía Solar Fotovoltaica, ENE2007-66135).*

## References

[1] Archana Bharathidasan and Sanjay Madria. Sensor networks: An overview. *IEEE Potentials*, 22(2):20–23, 2003.

[2] Rodney A. Brooks. Intelligence without representation. *Artificial Intelligence*, 47(1-3):139–159, 1991.

[3] Lifeng Chen, Zhanglong Chen, and Shiliang Tu. A realtime dynamic traffic control system based on wireless sensor network. In *ICPPW '05: Proceedings of the 2005 International Conference on Parallel Processing Workshops*, pages 258–264, Washington, DC, 2005. IEEE Computer Society.

[4] Peter M. Corcoran, Joe Desbonnet, Petronel Bigioi, and Ioan Lupu. Home network infrastructure for handheld/wearable appliances. *IEEE Transactions on Consumer Electronics*, 48(3):490–495, 2002.

[5] Alvaro Gutiérrez and Luis Magdalena. Control domótico de una vivienda sostenible basado en rs-485. In *UCAmI'2005: Proceedings of the I Symposium on Ubiquitous Computing and Ambient Intelligence*, pages 321–328, Madrid, Spain, 2005. Thomson Paraninfo.

[6] Christian Hofmann, Christian Weigand, and Josef Bernhard. Wireless medical sensor network with zigbee™. In *EHAC'06: Proceedings of the 5th WSEAS International Conference on Electronics, Hardware, Wireless and Optical Communications*, pages 12–15, Stevens Point, Wisconsin, USA, 2006. World Scientific and Engineering Academy and Society (WSEAS).

[7] Dimitrios Hristu-Varsakelis, William S. Levine, R. Alur, K.-E. Arzen, John Baillieul, and T. A. Henzinger. *Handbook of Networked and Embedded Control Systems (Control Engineering)*. Birkhauser, Boston, MA, 2005.

[8] Lingxuan Hu and David Evans. Localization for mobile sensor networks. In *MobiCom '04: Proceedings of the 10th annual international conference on Mobile computing and networking*, pages 45–57, New York, NY, 2004. ACM Press.

[9] I. Kelly and A. Martinoli. A scalable, on-board localisation and communication system for indoor multi-robot experiments. *Sensor Review*, 24(2):167–180, 2004.

[10] Shizuang Lin, Jingyu Liu, and Yanjun Fang. Zigbee based wireless sensor networks and its applicaions in industrial. In *Proceedings of the 2007 IEEE International Conference on Automation and Logistics*, pages 1979–1983, Piscataway, NJ, 2007. IEEE Press.

[11] M. Oca na, L. M. Bergasa, M. A. Sotelo, R. Flores, and R. Barea. Training method improvements of a wifi navigation system based on pomdp. In *Proceedings of the 2006 IEEE/RSJ International Conference on Intelligent Robots and Systems*, pages 5259–5264, Piscataway, NJ, 2006. IEEE Press.

[12] Ilker Onat and Ali Miri. An intrusion detection system for wireless sensor networks. In *WiMob'2005: Proceedings of the 2005 IEEE International Conference on Wireless And Mobile Computing, Networking and Communications*, pages 253–259, Piscataway, NJ, 2005. IEEE Press.

[13] D. Payton, M. Daily, R. Estowski, M. Howard, and C. Lee. Pheromone robotics. *Autonomous Robots*, 11(3):319–324, 2001.

[14] Rolf Pfeifer and Josh C. Bongard. *How the Body Shapes the Way We Think: A New View of Intelligence (Bradford Books)*. The MIT Press, Cambridge,MA, 2006.

[15] J. Pugh and A. Martinoli. Relative localization and communication module for small-scale multi-robot systems. In *IEEE International Conference on Robotics and Automation*, pages 188–193, Piscataway,NJ, 2006. IEEE Press.

[16] Gerhard Reitmayr, Ethan Eade, and Tom Drummond. Localisation and interaction for augmented maps. *ISMAR'05: Fourth IEEE and ACM International Symposium on Mixed and Augmented Reality*, 0:120–129, 2005.

[17] S.I. Roumeliotis and G.A. Bekey. Distributed multirobot localization. *IEEE Transactions on Robotics and Automation*, 18(5):781–795, 2002.

[18] Guangming Song, Zhigang Wei, Weijuan Zhang, and Aiguo Song. A hybrid sensor network system for home monitoring applications. *IEEE Transactions on Consumer Electronics*, 53(4):1434–1439, 2007.

[19] Luc Steels and Rodney Brooks. *The Artificial Life Route to Artificial Intelligence: Building Embodied, Situated Agents*. Lawrence Erlbaum Associates, Inc., Mahwah, NJ, 1995.

[20] Duc A. Tran and Thinh Nguyen. Localization in wireless sensor networks based on support vector machines. *IEEE Transactions on Parallel and Distributed Systems*, 19(7):981–994, 2008.

[21] Francisco J. Varela, Evan Thompson, and Eleanor Rosch. *The embodied mind*. MIT Press, Cambridge,MA, 1991.